UNLIMITED DISTRIBUTION

National Defence
Research and Development Branch

Défense Nationale
Bureau de Recherche et Développment

A TWO-ENDED SHOOTING TECHNIQUE FOR CALCULATING NORMAL MODES IN UNDERWATER ACOUSTIC PROPAGATION

Dale D. Ellis

September 1985

Approved by R.F. Brown Director/Underwater Acoustics Division

DISTRIBUTION APPROVED BY

CHIEF D.R.E.A.

REPORT 85/105

Defence Research Establishment Atlantic

Centre de Recherches pour la Défense Atlantique

Canada

ABSTRACT

An algorithm for the calculation of acoustic normal modes in the ocean is described. The algorithm is valid for an arbitrary sound speed and density profile in the water column and bottom. Losses due to volume absorption in the water and bottom, surface and bottom roughness, and shear waves in the bottommost layer can be calculated as perturbations.

The essential feature of the algorithm is a two-ended shooting method in which the trial solution is started separately at the surface and bottom and numerically integrated to a matching depth in the middle, usually near the minimum sound speed. The trial solution is iterated until a continuous function with a continuous derivative is obtained. Shooting from both ends results in a more stable algorithm and gives more accurate eigenfunctions than are obtained using conventional single-ended shooting methods.

This paper describes the theory and general numerical implementation of the algorithm. For completeness, equations are given for calculating group velocities, propagation loss in a range-dependent environment, and losses due to volume absorption, surface and bottom roughness, and shear waves in the bottommost layer.

The two-ended shooting algorithm has been implemented in the computer program PROLOS, which has been used extensively at DREA since 1979. In this paper results of numerical computations will be presented, including the AESD Workshop Test Cases and comparison of predictions with some measured data from a shallow water propagation loss experiment.

RESUME

On décrit un algorithme de calcul des modes acoustiques normaux en mer. L'algorithme est applicable à un profil arbitraire de densité et de vitesse du son dans la colonne d'eau et au fond. Les affaiblissements dus à l'absorption par la masse de l'eau et du fond, à la rugosité de la surface et du fond et aux ondes de rotation dans la couche inférieure peuvent être traités comme des perturbations.

L'élément essentiel de cet algorithme est une méthode de "tir" bilatéral dans laquelle la solution d'essai est appliquée séparément à la surface et au fond et est intégrée numériquement jusqu'à une profondeur de rencontre au milieu, habituellement près du point de vitesse du son minimum. On améliore par itération la solution d'essai jusqu'à ce qu'on obtienne une fonction continue avec une dérivée continue. Le "tir" bilatéral donne un algorithme plus stable et des fonctions propres plus précises que les méthodes habituelles de "tir" unilatéral.

Le présent document contient des renseignements sur la théorie et le calcul numérique général de l'algorithme. Pour plus de clarté, on donne les équations de calcul des vitesses de groupe, de l'affaiblissement par propagation en fonction de la distance et des affaiblissements dus à l'absorption par la masse, à la rugosité de la surface et du fond et aux ondes de rotation dans la couche inférieure.

L'algorithme de "tir" bilatéral a été intégré au programme informatique PROLOS qui a été largement utilisé au CRDA depuis 1979. Dans le présent document, on donne les résultats des calculs numériques, y compris ceux des cas types de l'atelier AESD, et on compare des valeurs prévues avec certaines mesures tirées d'une expérience d'affaiblissement par propagation en eau peu profonde.

TABLE OF CONTENTS

1. INTRODUCTION

To predict underwater acoustic propagation from a knowledge of the environment, a number of models - primarily ray theoretic and normal modes - have been introduced. Such models have been applied to a variety of cases: deep and shallow water, high and low frequency, range-independent and range-dependent environments. For shallow water studies normal mode models have been found to be the most appropriate, particularly at frequencies below 1 kHz. Until 1978, DREA had been using a version of the normal mode program by Bartberger and Ackler [1973] of the United States Naval Air Development Center. Since this program was written originally for a CDC computer, its conversion to run on a DEC-20 system revealed two numerical problems - overflow of exponent and loss of precision. Both problems arose from the shooting technique used to solve for the normal mode wave numbers and mode functions. Although the program could have been recoded to overcome these deficiencies, an improved algorithm was developed.

This paper describes the alternate algorithm which avoids both the exponent overflow and the loss of precision of the Bartberger shooting algorithm by using a two-ended shooting technique instead of a single-ended method. It is also quite general in that an arbitrary sound speed and density profile can be handled. Loss mechanisms, such as volume attenuation in the water and bottom, surface and bottom roughness, and shear waves can be incorporated as perturbations. The formulation is given in terms of the pressure rather than the velocity potential, since the former allows density changes to be more conveniently handled, and pressure is a measurable quantity.

The discussion that follows will first give a short description of normal mode theory and present the equations for the normal modes and the perturbative losses. For completeness the equations for calculating group velocities and propagation loss in a range-dependent environment are also included. This is followed by a description of the two-ended shooting method as it applies to normal mode calculations in underwater acoustics. The necessary equations are presented and cast in dimensionless co-ordinates for use in computations.

The numerical algorithm can be implemented in a number of ways. Two computer codes have been developed and have been used extensively in the shallow water studies at DREA. One [Ellis and Leverman, 1982] uses a layered environmental model similar to Bartberger; another [MacEachern, 1983] uses a combination of the Noumerov method and a Runge-Kutta ordinary differential equation solver. Results of numerical computations are also presented, including the ABSD Workshop test cases [Spofford, 1973] and comparison of predictions with some measured data from a shallow water site.

2. THEORETICAL BACKGROUND

2.1 The Normal Mode Equations

The environment that can be handled by normal mode theory is depicted in Fig. 1. It consists of a stratified medium in which the sound speed and density can vary arbitrarily with depth, but which do not change with range. In its exact form the boundaries must be smooth and the medium must not be lossy. However, it is possible using perturbation methods to extend the theory to include the effects of volume absorption in the water and bottom, scattering from rough boundaries, weak range-dependence, and shear waves in the bottommost layer. For a CW point source of frequency f operating at range r=0 and depth z_o, the pressure field P at an arbitrary depth z and horizontal range r from the source is given by:

$$P(r,z,t) = \frac{i\pi S}{\rho(z_o)} \sum_{n=1}^{N} u_n(z_o)\, u_n(z)\, H_o^{(1)}(k_n r)\, e^{-i\omega t} + \text{continuous spectrum.} \qquad (1)$$

In the above equation, S is the source strength (see below), ρ is the density, N is the number of trapped modes, the u_n are the normal mode functions, $H_o^{(1)}$ is the Hankel function of zeroth order and first kind, k_n is the horizontal wave number of the nth mode, $\omega=2\pi f$ is the angular frequency of the source, and t is the time. The time dependence is not important for what follows so will be dropped for notational simplicity. In order for modes to be trapped, the bottommost layer must have a sound speed which is greater than the minimum sound speed. A rough estimate of the number of trapped modes is $N \approx hf/c_m$, where c_m is the minimum sound speed and h is the water depth. A better approximation [Ellis, 1982], derived using WKB theory [e.g., Schiff, 1968] and neglecting density changes, is:

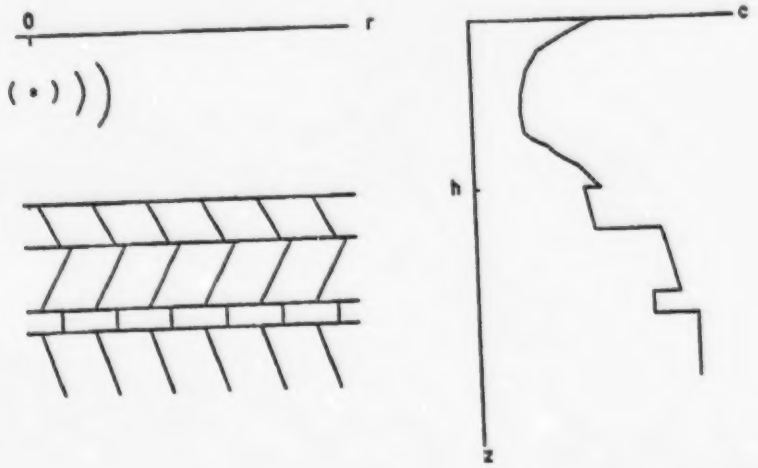

Fig. 1. The normal mode environmental model. Both sound speed and density can vary arbitrarily and discontinuously with depth.

$$N = [[\tfrac{1}{2} + (2hf\eta/c_m)(1 - c_m^2/c_B^2)^{1/2}]] \tag{2}$$

where [[x]] is used to denote the integer of part of x, c_B is the sound speed in the bottommost layer (extending from depth z_B to ∞), and η is a dimensionless quantity which depends only on the shape of the sound speed profile. The values of η are usually in the range 0.5 to 1.0. As examples, η=1 for a two-isovelocity layer model, η=0.79 for a parabolic profile, and η=0.67 for a bilinear profile.

If N > 1, the continuous spectrum usually gives negligible contribution to the pressure at ranges greater than several water depths, and is usually neglected in calculations.

There are a number of conventions for what is meant by a source of unit strength. The convention implied by Eq. (1) is that the pressure is unity at a unit distance from the source; that is, near the source the pressure is given by:

$$P(\underline{x},t) = S|\underline{x}-\underline{x}_o|^{-1} \exp[i(k_o|\underline{x}-\underline{x}_o| - \omega t)] \tag{3}$$

where $\underline{x} = (r,z)$, $k_o = \omega/c_o$, and c_o is the sound speed at the source position x_o. S has numerical value of unity, but has the appropriate units of pressure times length.

Once the pressure has been obtained using Eq. (1), the propagation loss can be obtained from:

$$PL = -10 \log_{10}|P/P_{ref}|^2 \tag{4}$$

where P_{ref} is the pressure at unit distance from the source. Combining Eqs. (1), (3) and (4) gives the expression for propagation loss in terms of the normal modes and wave numbers:

$$PL(r,z) = -10 \log_{10}\left|\frac{\pi}{\rho(z_o)} \sum_{n=1}^{N} u_n(z_o)\, u_n(z)\, H_o^{(1)}(k_n r)\right|^2. \tag{5}$$

To obtain the pressure field, Eq. (1), it is necessary to solve the normal mode equation to obtain the normal mode eigenvalues k_n^2 and eigenfunctions $u_n(z)$. They are the solutions to the second order differential equation:

$$\rho(z)\frac{d}{dz}\left[\frac{1}{\rho(z)}\frac{du_n(z)}{dz}\right] + \left[\frac{\omega}{c^2(z)} - k_n^2\right] u_n(z) = 0 \tag{6}$$

and satisfy the conditions:

(i) $u_n(z)$ is continuous, which corresponds physically to the pressure being continuous.

(ii) $(du_n/dz)/\rho(z)$ is continuous, which corresponds to the vertical particle velocity being continuous.

(iii) $u_n(0)=0$, which corresponds to zero pressure at the ocean surface.

(iv) The trapped modes have finite normalization. If the bottommost layer has a constant density and sound speed, the trapped modes behave as:

$$u_n(z) \sim A \exp[(k_n^2 - \frac{\omega^2}{c_B^2})^{1/2} z] . \tag{7}$$

Under the above conditions, there are a discrete set of solutions to Eq. (6), with wave numbers k_n constrained by:

$$\frac{\omega}{c_m} > k_1 > k_2 > \ldots > k_N > \frac{\omega}{c_B} . \tag{8}$$

The normal mode functions are orthogonal with respect to the weighting function ρ^{-1} and are normalized to unity, that is:

$$\int_0^\infty \frac{1}{\rho(z)} u_m(z)\, u_n(z)\, dz = \delta_{mn} \tag{9}$$

where δ_{mn} is the Kronecker delta.

2.2 Modal Loss Calculations

If any form of loss is introduced into the system, the normal mode wave numbers become complex with a small imaginary component; that is:

$$K_n = k_n + i\,\delta_n \tag{10}$$

where K_n is now the complex wave number. The expressions for the pressure and propagation loss are unchanged except that K_n now replaces k_n. If the losses are small, they can be treated as perturbations of the lossless normal mode solutions. The imaginary part δ_n is the sum of the various attenuation mechanisms:

$$\delta_n = \delta_n^{\text{bottom}} + \delta_n^{\text{water}} + \delta_n^{\text{scatt}} + \delta_n^{\text{shear}} + \ldots \tag{11}$$

where δ_n^{bottom} is the loss due to volume absorption in the bottom layers, δ_n^{water} is the loss due to volume absorption in the water column, δ_n^{scatt} is the loss from the coherent field due to scattering from rough surfaces, and δ_n^{shear} is the loss due to shear waves in the bottommost layer. Expressions for the losses are given below.

2.2.1 Bottom absorption

The volume absorption coefficient α for the bottom layers experimentally seems to be linearly dependent on frequency [Hamilton, 1974] and is often given in the units dB/length at 1 kHz. Thus, at a given frequency, the absorption coefficient is:

$$\epsilon = \frac{\alpha f/1000}{20 \log_{10} e} \tag{12}$$

which has units of nepers/length, or simply inverse length, the same as the wave number k_n.

For a bottom with an arbitrary sound speed, density and absorption profile, the attenuation coefficient due to volume absorption is given by:

$$\delta_n^{bottom} = (\omega/k_n) \int_h^{\infty} \frac{\epsilon(z)\, u_n^2(z)}{\rho(z)\, c(z)}\, dz. \tag{13}$$

The derivation of this formula is given in Appendix B. The attenuation due to any layer can be obtained by restricting the range of integration to that layer. If the bottommost layer supports shear waves, then it is not included in the integration; the equations of Sec. 2.2.4 are used instead.

2.2.2 Volume absorption in the water column

The attenuation due to absorption of acoustic energy by the water column can be treated in an identical manner to the absorption by the bottom layers. However, the plane wave absorption coefficient varies as f^2 rather than linearly as for the sediments. The absorption coefficient at any frequency can be obtained from a formula such as Thorpe's [1967]:

$$\alpha_w = \left[\frac{0.1\, f^2}{1 + (f/1000)^2} + \frac{40\, f^2}{4100 + (f/1000)^2}\right] \frac{10^{-9}}{0.9144}. \tag{14}$$

α_w has units of dB/meter. The corresponding modal attenuation coefficient is then (Appendix B):

$$\delta_n^{\text{water}} = (\omega\, \varepsilon_w / \rho_w k_n) \int_o^h \frac{u_n^2(z)}{c(z)}\, dz \qquad (15)$$

where ρ_w is the density of water and where:

$$\varepsilon_w = \alpha_w / 20 \log_{10} e.$$

2.2.3 Surface and bottom scattering

Scattering losses due to rough boundaries can be included in an approximate way. By ignoring the contribitions from the non-specularly reflected energy, and using the Kirchhoff approximation, Kuperman and Ingenito [1977] find the modal attenuation coefficient for surface and bottom roughness to be:

$$\delta_n^{\text{S-scatt}} = \frac{\sigma_o^2 \gamma_n(o)}{2\rho(o) k_n} \left[\frac{du_n(o)}{dz}\right]^2 \qquad (16)$$

$$\delta_n^{\text{B-scatt}} = \frac{\sigma_1^2 \gamma_n(h^-)}{2\rho(h^-) k_n} \left\{\left[\frac{du_n(h^-)}{dz}\right]^2 + [\gamma_n(h^-) u_n(h^-)]\right\}^2 \qquad (17)$$

where

$$\gamma_n(z) = (\omega^2/c^2(z) - k_n^2)^{1/2}.$$

σ_o and σ_1 are the r.m.s. surface and bottom roughness heights, and the notation h^- means that the various functions are to be evaluated just above the water-bottom interface. Also note that if $\omega/c(o) \leq k_n$ or $\omega/c(h^-) \leq k_n$, then the corresponding scattering losses are zero.

These formulae are valid in the small wave height approximation:

$$2\sigma_o^2 \gamma_n^2(o) \ll 1,$$

and $$2\sigma_1^2 \gamma_n^2(h^-) \ll 1. \qquad (18)$$

2.2.4 Shear waves in the bottommost layer

When the speed of shear waves in the bottommost layer c_s is considerably less than the minimum speed of the compressional waves at all depths, the losses can be treated by perturbation methods. A formula is given in a report on the SNAP normal mode program [Jensen and Ferla, 1979]:

$$\delta_n^{\text{shear}} = \frac{u_n^2(z_B^+)}{\rho_2} \frac{\beta_1}{8k_n} \left[1 + \left(\frac{\rho_1}{\rho_2} \frac{\beta_1}{\beta_2}\right)^2\right] Q(\beta_1) \tag{19}$$

where $z_B^{\pm}$ refer to points just above (-) and just below (+) the top of the bottommost layer,

$$\beta_1 = \left(\frac{\omega^2}{c^2(z_B^-)} - k_n^2\right)^{1/2},$$

$$\beta_2 = \left(k_n^2 - \frac{\omega^2}{c^2(z_B^+)}\right)^{1/2},$$

and

$$Q(\beta_1) = \begin{cases} 1 - |R|^2 & \text{if Real } \beta_1^2 \geq 0 \\ 2\,\text{Imag}(R) & \text{if Real } \beta_1^2 < 0\,. \end{cases} \tag{20}$$

$R(\beta_1)$ is the plane wave reflection coefficient [Brekhovskikh, 1980],

$$R(\beta_1) = \frac{\rho_2 \beta_1 C_{2s} + \rho_2 (\beta_1 \beta_2 / \beta_s) S_{2s} - \rho_1 \beta_2}{\rho_2 \beta_1 C_{2s} + \rho_2 (\beta_1 \beta_2 / \beta_s) S_{2s} + \rho_1 \beta_2} \tag{21}$$

where

$$\beta_s = \left(\frac{\omega^2}{c_s^2} - k_n^2\right)^{1/2},$$

$$C_{2S} = [1 - 2(k_n c_s/\omega)^2]^2$$

$$S_{2S} = 1 - C_{2S}.$$

Note that this formula contains losses due to both the compressional and shear wave losses.

2.3 Group Velocities

The speed at which acoustic energy is transported in mode n at frequency ω is given by the group velocity $v_g^{(n)} = |d\omega/dk_n|$. This expression is often evaluated by solving the normal mode Eq. (6) at two frequencies $\omega \pm \Delta\omega$ and forming the finite difference estimate $\hat{v}_g^{(n)} = |\Delta\omega/\Delta k_n|$. However, in addition to the extra computational effort, the technique is subject to numerical error.

An exact and alternate expression for the group velocity [Tolstoy, 1956; Koch et al, 1983] is given by:

$$v_g^{(n)} = \left[\frac{\omega}{k_n} \int_0^\infty \frac{u_n^2(z)}{\rho(z)\, c^2(z)}\, dz\right]^{-1}. \qquad (22)$$

This formula is similar to the expression for the volume attenuation coefficient [Appendix B], and can be derived in a similar manner [Chapman and Ellis, 1983]. Because of the similarity of the above integral with Eqs. (13) and (15), the group velocity can be obtained with essentially no additional computation.

2.4 Extensions for Comparison with Data

The expressions for the pressure and propagation loss, Eqs. (1) and (5), can be easily extended to facilitate comparison with measurements in a weakly range-dependent environment and for a broadband source.

The expression for the propagation loss given in Eq. (5) is a coherent summation of the modes that includes all the interference terms. It is sometimes more appropriate to sum the modes incoherently to obtain:

$$IPL(r,z) = -10 \log_{10}\{[\pi/\rho(z_o)]^2 \sum_{n=1}^{N} |u_n(z_o)\, u_n(z)\, H_o^{(1)}(k_n r)|^2\}.$$

This is a smooth function of range since:

$$|H_o^{(1)}(k_n r)|^2 \sim (2/\pi k_n r)\, e^{-2\delta_n r}$$

where the asymptotic form of the Hankel function has been used, and the mode attenuation δ_n, Eq. (10), has been included. The neglected terms in the propagation loss are of the form:

$$(2/\pi r) \sum_{\substack{n,m=1 \\ n\neq m}}^{N} u_n(z_o)\, u_n(z)\, u_m(z_o)\, u_m(z)\, (k_n k_m)^{-1/2} \exp[i(k_n - k_m)r - (\delta_n + \delta_m)r]$$

which are expected to be small for a number of reasons. First, the oscillating terms $\exp[i(k_n - k_m)r]$ will tend to make the range-averaged value small. Second, if averaged over a frequency band, there will be additional smoothing.

The incoherent propagation loss should be used cautiously for deep water environments since the regions of high and low intensity including convergence zones are averaged out. However, in shallow water it is a useful quantity, and for broadband sources is more meaningful than the coherent propagation loss.

For an environment in which the sound speed profile and water depth are slowly varying, mode coupling can be neglected and the adiabatic approximation holds [Pierce, 1965]. The form of the expressions for the pressure and propagation loss is unchanged except that:

(i) $u_n(z_o)$ is obtained from the environment at range r=0;

(ii) $u_n(z)$ is obtained from the environment at range r;

(iii) k_n is the average value of the wave number in the range 0 to r; and,

(iv) the number of modes is determined from the minimum value of N at all ranges between 0 and r.

In principle, the normal modes should be calculated at every range for which the propagation loss is desired. In practice, the mode functions and wave numbers are evaluated at a relatively small number of ranges and interpolated for intermediate ranges.

8. NUMERICAL IMPLEMENTATION

A common procedure for solving for the normal mode eigenfunctions and eigenvalues is to numerically integrate the normal mode Eq. (6) using a shooting method. In this method a trial value is chosen for k_n, then starting at some large value of z deep in the ocean bottom with suitable values of u and du/dz, the solution is numerically integrated toward the ocean surface* at z=0. In general, the solution obtained from the trial value of k_n will not satisfy the condition $u_n(0)=0$, but based on the calculated values of u and u' at z=0 a new value of k_n can be estimated. The procedure is repeated until the value of u_n at z=0 is sufficiently small, or until k_n has the required degree of accuracy.

8.1 Some Difficulties With Shooting Methods

Two numerical problems can occur with this method of shooting, namely, exponent overflow and loss of precision. In solving the normal mode equation in underwater acoustics, exponent overflow will occur if the starting point is chosen too deep, that is if z is too large. Although less likely near the surface, it can also occur there if the sound speed increases near the surface, that is if $c>\omega/k_n$. The increase in sound speed near the surface can cause a second problem as well - loss of precision - because the true solution gets increasingly buried in the roundoff and truncation errors as the integration proceeds toward the ocean surface. These difficulties will be discussed later in more detail, and a method will be proposed for getting around these problems.

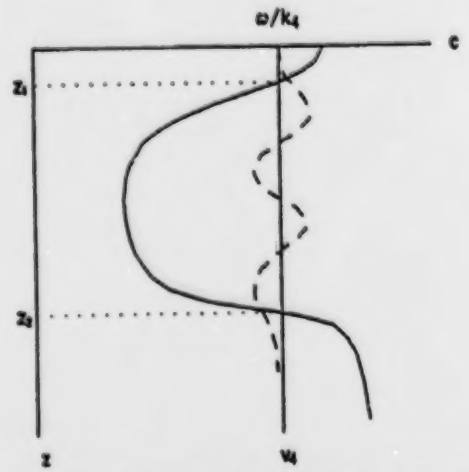

Fig. 2. Normal mode solution $u_4(z)$ (dashed line) superimposed on a sound speed profile c(z) (solid line).

---

*One cannot start at the surface and integrate downward into the bottom because numerical roundoff would cause the functions to grow exponentially even for the "exact" k_n where the functions should decay exponentially.

Before elaborating on these points, however, it is useful to look at some properties of the mode function. Fig. 2 shows a mode function superimposed on a sound speed profile at the phase velocity $v_n = \omega/k_n$ of the mode. A number of properties of the mode function to note are as follows: from the boundary condition at the surface,

(1) $u_n(0)=0$;

and from γ_n as defined following Eq. (17),

(2) for $z < z_1$, then $\gamma_n^2 < 0$, and $u_n(z)$ has an increasing exponential type of behaviour. The solution is approximately given by:

$$u_n(z) = \exp[I_1(z)] - \exp[-I_1(z)] \tag{23}$$

where,

$$I_1(z) = \int_0^z |\gamma_n(z)|\, dz$$

(3) for $z_1 < z < z_2$, then $u_n(z)$ is oscillatory. The solution is approximately given by:

$$u_n(z) = A(z) \sin(I_2(z) + \phi) \tag{24}$$

where,

$$I_2(z) = \int_{z_1}^z \gamma_n(z)\, dz$$

A(z) is slowly varying, and ϕ is the phase, approximately $\pi/4$, at the turning point z_1.

(4) for $z > z_2$, $u_n(z)$ has a decreasing exponential type of behaviour. The boundary condition at infinity requires that only the decreasing exponential be present; thus,

$$u_n(z) = C \exp[-I_3(z)] \tag{25}$$

where C is a real constant, and

$$I_3(z) = \int_{z_2}^z |\gamma_n(z)|\, dz. \tag{26}$$

(5) In the interval $z_1 < z < z_2$, $u_n(z)$ has n-1 zeros.

The numerical problems occur in the exponential regions. Suppose we started at z=0 and integrated the differential equation downwards toward z_1. Although the increasing and decreasing terms have equal amplitude at z=0, the increasing exponential soon dominates and the second term gets lost in the roundoff error. Any error that occurs in the coefficient of $\exp[-I_1(z)]$ is soon damped out, and the method is stable. The only problem that might occur is that I(z) becomes large enough so that exp[I(z)] may cause overflow in computer calculations. On the other hand, suppose that we have the correct solution at $z=z_1$ and want to integrate (shoot) upwards toward z=0; the procedure leads to loss of precision. Suppose there is a slight roundoff so that the coefficient of $\exp[-I_1(z)]$ is no longer unity but 1+ε, where ε is a very small quantity. Even with no further roundoff, the solution is no longer zero but:

$$u_n(o) = -\varepsilon \exp[I_1(z_1)] \tag{27}$$

so we have lost $I_1(z_1)\ln(10)$ significant digits in the accuracy of the mode function. This in turn will cause problems in the algorithm that predicts the next trial value of k_n. [The final accuracy of k_n is not necessarily degraded, since the numerical procedure can be terminated as long as k_n is sufficiently accurate, even though the condition $u_n(0) <$ tolerance is not satisfied. However, convergence may be slower, and the mode function will be less accurate for $z < z_1$; that is, near the surface where solutions are very often needed.] This loss of accuracy can be eliminated by integrating downward from z=0. Similarly, the solution for large values of z can be accurately obtained by integrating upward toward the surface. The numerical problems do not occur for $z > z_2$ since we are integrating upwards and any part of the unwanted solution gets quickly damped out.

The method of matching the upward and downward solutions and getting an improved estimate for the eigenvalue is discussed in the next section.

8.2 The Two-Ended Shooting Method

The previously discussed loss of precision encountered in the single-ended shooting method can be remedied by using a two-ended shooting method. The problem of exponent overflow in numerical computations is easily handled, so discussion is postponed until later. We first discuss the two-ended shooting method and the iteration procedure for refining the accuracy of the trial eigenfunction, or wave number.

The method described here is a generalization of that of Blatt [1967] for the solution of the Schrödinger equation of quantum mechanics. The generalization allows for density changes in the acoustic medium, a feature that does not occur in the quantum mechanical problem. The generalized algorithm which is used to refine the approximate eigenvalue is obtained from an application of the variational principle, and is derived in Appendix C.

3.2.1 Outline of the shooting method

A brief sketch of the two-ended shooting method will now be presented using Fig. 2 for reference. First, a matching depth z_m is chosen between the turning points z_1 and z_2; a convenient choice for this depth is the minimum sound speed, since the solution is always oscillatory at the minimum sound speed. Next, an estimate is made for the eigenvalue k_n^2 and the turning points z_1 and z_2 are determined. Then, suitable limits of integration z_a and z_b are determined. In practice these limits are often the ocean surface and the top of the bottommost layer, respectively. Suitable boundary conditions are chosen at z_a and z_b and the differential equation is integrated (down) from z_a to the matching depth z_m, and (up) from z_b to z_m. The integration procedure gives the function u_n and its derivative at z_m from the two integrations. Since the normalizations are arbitrary, one of the mode functions can be renormalized to give a function which is continuous, but which in general has a discontinuous derivative. Provided the number of zero crossings of the mode function is correct, an improved approximation for the eigenvalue k_n^2 is given by (Appendix C):

$$k_n^2 \to k_n^2 + \frac{\left[\frac{1}{\rho(z_m^-)}\frac{du_n(z_m^-)}{dz} - \frac{1}{\rho(z_m^+)}\frac{du_n(z_m^+)}{dz}\right] u_n(z_m)}{\int_{z_a}^{z_b} \frac{u_n^2(z)}{\rho(z)}\,dz}. \qquad (28)$$

The above equation is the key formula for the improvement of the eigenvalue. The notation z_m^- or z_m^+ means that the functions ρ or u_n are to be evaluated just above (-) or just below (+) the matching depth z_m. The procedure is repeated until the correction term is small enough, and/or until the derivatives match to sufficient accuracy. Since the method is derived using the variational principle, it is a second order method and converges rapidly.

3.2.2 The initial guess for the eigenvalue

The second order eigenvalue iteration procedure described above will only work if the trial mode function has the correct number of zero crossings. Thus, some other method must be used to get an approximate value for the eigenvalue in the correct range. For the first mode the WKB method could be used to get an approximate value for k_n, or a crude trial function could be used with the variational principle. An even cruder method is simply to take ω/c_B and ω/c_m as limits for k_1 and to use the shooting method together with a binary search. If

there are too many zero crossings of the mode, the trial value of k_n is too small; if there are too few zero crossings, the trial value is too large. The range of possible values for k_n is halved at each iteration. Once the number of mode crossings is correct the faster second order method can be used.

For higher modes the upper limit on k_n is the wave number of the mode (n-1). The lower limit is not as easy to determine, although ω/c_B could always be used. For an isovelocity profile, which is the worst case, an approximation to k_n is given by:

$$k_n^2 = k_{n-1}^2 - \frac{2\pi}{h}^2 (n-2) . \tag{29}$$

Thus, if we take the upper limit from the above equation, with a safety factor of two for good measure multiplying the second term on the right, we should be safe. A conservative estimate for the lower limit of k_n is thus:

$$k_n^{min} = \max \{ \frac{\omega}{c_B}, [k_{n-1}^2 - \frac{4\pi^2}{h^2} (n-2)]^{1/2} \} . \tag{30}$$

The trial value of k_n for higher modes can be an extrapolation procedure based on the values of k_n for the previous two or three modes.

3.2.3 The number of trapped modes

At a given frequency the number of modes trapped by a given profile can be determined by applying the shooting method once, with a trial value of k_N equal to ω/c_B. The number of zero crossings are then counted and the correction of Eq. (28) applied to k_n. If the new value of k_N is greater than ω/c_B then the mode is trapped; i.e. there are N modes. If the new value of k_N is less than ω/c_B, only N-1 modes are trapped.

This procedure can also be used to determine which modes have a phase velocity less than some specified phase velocity. By applying the procedure twice, the number of modes between two phase velocities can be calculated.

3.2.4 Prevention of exponent overflow

In the shooting procedure, the integration limits z_a and z_b must be chosen so that the function $u_n(z)$ is effectively zero for $z < z_a$ and $z > z_b$. This can be done approximately by evaluating the WKB integral:

$$I(z) = \int_{z_t}^{z} |\gamma(z)|\, dz \tag{31}$$

where z_t is one of the turning points z_1 or z_2, γ has been defined earlier, and the integral is evaluated upward from z_1 or downward from z_2. The numerical integration does not have to be performed with any great accuracy, so the trapezoidal rule is sufficiently accurate. When the value of the integral has reached some value, say D, then the mode function will be reduced in amplitude by a factor of exp(D) compared with its value at the turning point. The depth z_a or z_b at which the integral exceeds D is then used for the starting point for the (accurate) numerical integration of the differential equation.

3.2.5 Initial values for the shooting procedure

To obtain mode functions which have an approximate value of unity at the turning points, suitable values of u and u' should be chosen at z_a and z_b.

Near the surface or z_a:

$$u(z_a) = \min\{\frac{1}{\sinh[I_1(z_a)]}, 1\} \qquad \text{if } z_a = 0 \text{ and } z_1 > 0 \tag{32}$$

$$u(z_a) = \exp[-I_1(z_a)] \qquad \text{if } z_a > 0 \tag{33}$$

In either case,

$$u'(z_a) = \gamma(z_a)\, u(z_a). \tag{34}$$

In the bottom, since the solution behaves as $\exp[-I_s(z)]$, the starting conditions are:

$$u(z_b) = \exp[-I_s(z_b)] \tag{35}$$

$$u'(z_b) = -\gamma(z_b)\, u(z_b). \tag{36}$$

3.3 Discussion

If the speed of sound at the surface is greater than the phase velocity of the mode; i.e. $[\omega/c(o)]<k_n$, then the two-ended shooting method is superior to one-ended shooting methods. Also, if the sound speed profile is such that $[\omega/c(0)]>k_n$, then the two-ended shooting method offers no disadvantages over the one-ended shooting methods; (unless, the eigenvalue refinement procedure of Eq. (28) happens to be superior). If the sound speed profile has two or more local minima, as would occur for example in a surface duct, then for modes which have several turning points, loss of precision will occur in integrating between the two minima. This loss of precision will be about the same no matter how we integrate through the sound speed maximum, whether by a one- or a two-ended shooting method. However, the two-ended method has the advantage that any loss of precision near the surface is avoided, and moreover the method described in Sec. 3.2 has promise for isolating the two regions if necessary. Thus, there seems to be no penalty in using the two-ended shooting method and for many sound speed profiles greater precision and stability can be achieved compared to the conventional single-ended shooting methods.

4. RESULTS

Two computer codes have been developed which use the two-ended shooting technique. One PROLOS/MODES [Ellis and Leverman, 1982; Leverman, 1982] uses a layered environmental model similar to Bartberger [1973]; PROLOS has been used extensively at DREA since 1979. A more recent program PRLOSS/NORMOD [MacEachern, 1983] uses a combination of the Noumerov method and a Runge-Kutta ordinary differential equation solver.

In this section we present some results based on using these models: the ABSD Workshop Test Cases, mode loss calculations, group velocity calculations, and comparison with shallow water propagation loss measurements.

4.1 ABSD Workshop Test Cases

Figs. 3a-3c, show the profiles used as test cases for the ABSD Workshop on low frequency modelling [Spofford, 1973]. Some of them are quite difficult tests of normal mode programs. The original tests had units of feet and feet per second; here they have been converted to metric using the exact conversion factor of 0.3048 m per foot.

Fig. 3. Sound speed profiles for the AESD Workshop Test Cases.

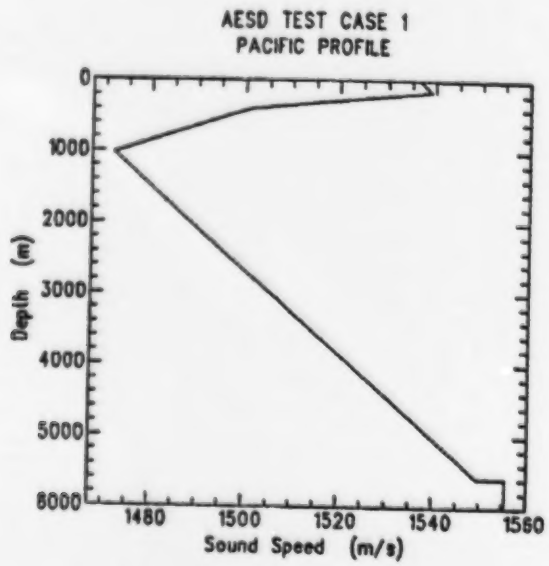

3(a) - Test Case 1: Pacific profile.

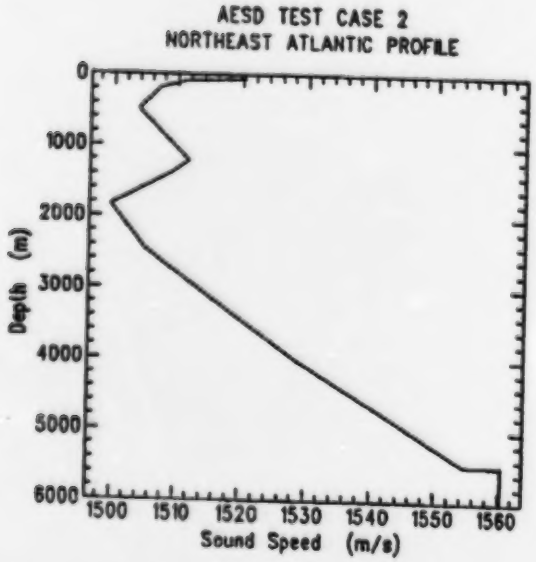

3(b) - Test Case 2: Northeastern Atlantic profile.

Fig. 3 (Cont'd)

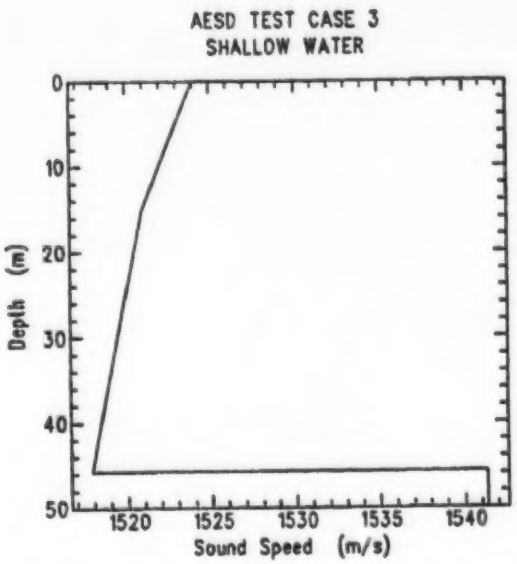

3(c) - Test Case 3: Shallow water profile.

Figs. 4a-4e show the propagation loss calculations for five test cases: two frequencies 300 and 25 Hz for Test Case 1, one frequency for Test Case 2, and two frequencies 500 and 50 Hz for Test Case 3. Calculations were performed using the PROLOS/MODES normal mode program, with 500 homogeneous layers of equal thickness in the water column. The sound speed used in each layer was obtained by first interpolating between the input profile points so that $c^{-2}(z)$ was linear, then using the average value of the interpolated sound speed in each layer. No earth curvature correction, absorption losses, or other losses are included in the calculations. Calculation times were about 4 to 5 seconds per mode on a DEC-2060 computer for eigenvalue accuracies of 15 digits. Typically only about 5 iterations of the second order method, Eq. (28), are required.

As mentioned above, some of these test cases are quite difficult tests of normal mode models, and there is considerable variation in the results presented at the AESD Workshop [Spofford, 1978]. Indeed many of the normal mode programs could not handle all the tests. There do not seem to be benchmark solutions for most of these cases but our predictions are in reasonable agreement with other models. The only difficulty we encountered with these profiles was in Test Case 2, the northeast Atlantic profile, which has two major sound channels separated by a local sound speed maximum. In this case the mode function 4 fails to converge after 30 iterations although the wave number seems accurate. The problem seems to be due to the fact that the mode has a large amplitude in the upper duct, and a small amplitude in the lower duct where the matching depth was chosen.

Fig. 4. Propagation loss versus range for the AESD Workshop Test Cases.

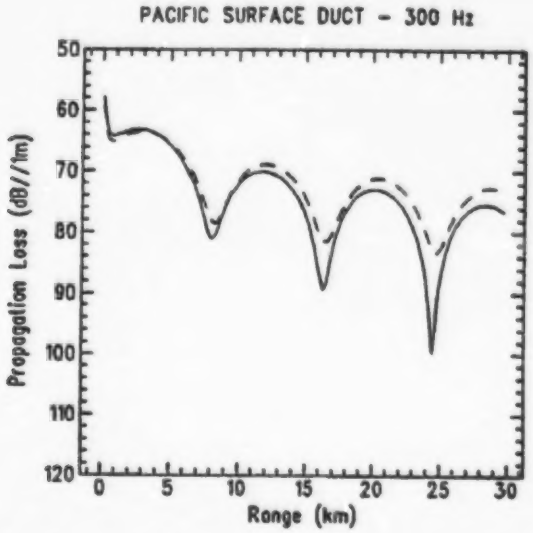

4(a) - Test Case 1A: frequency 300 Hz, source depth 91.44 m, receiver depth 27.432 m. The solid line is for the surface channel only with a half-space below; the dashed line is for the entire profile but with modal phase velocities confined to the range 1536 to 1539.24 m/s.

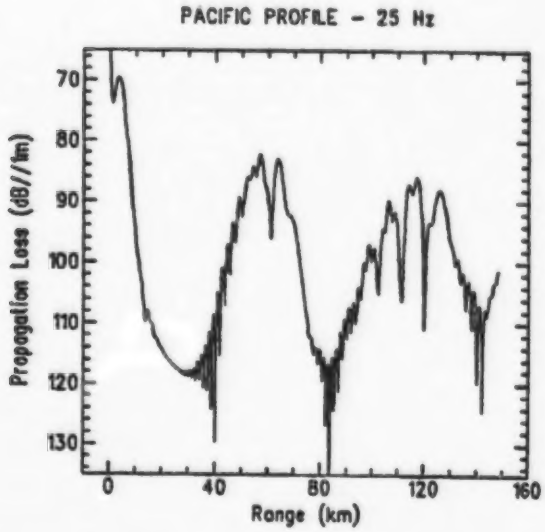

4(b) - Test Case 1B: frequency 25 Hz, source depth 253.8984 m, receiver depth 863.4984 m.

Fig. 4 (Cont'd)

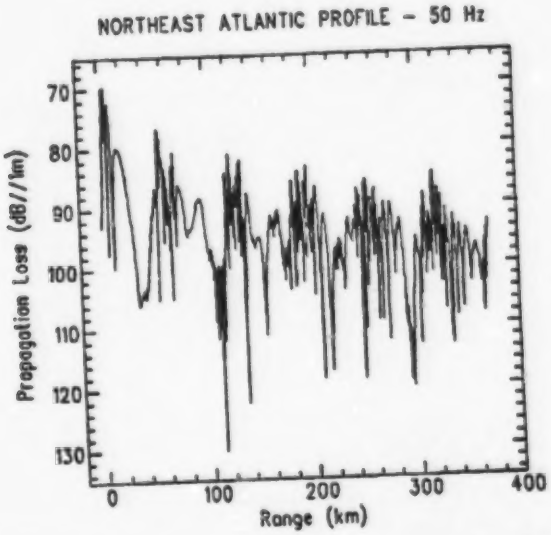

4(c) - Test Case 2: frequency 50 Hz, source depth 243.84 m, receiver depth 1097.28 m.

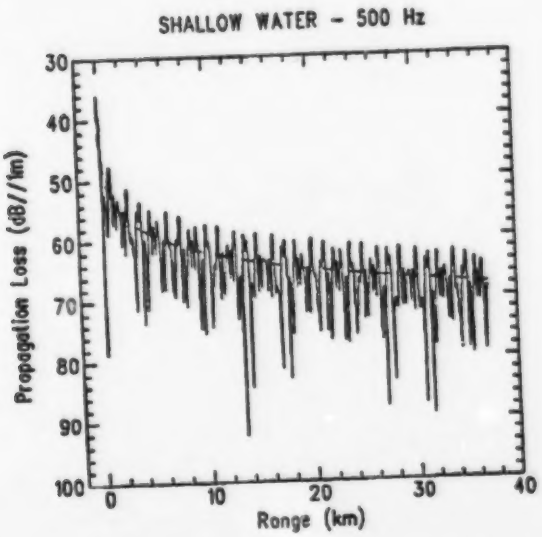

4(d) - Test Case 3A: frequency 500 Hz, source depth 6.096 m, receiver depth 12.192 m. The dashed line shows the loss when the modes are summed incoherently.

Fig. 4 (Cont'd)

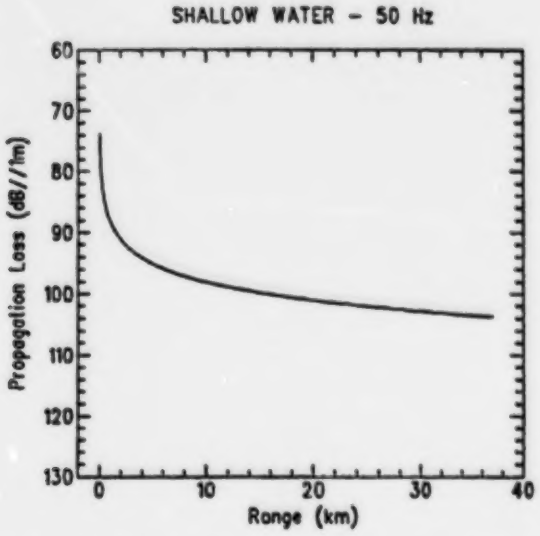

4(e) - Test Case 3B: frequency 50 Hz, source depth 6.096 m, receiver depth 12.192 m.

Of particular interest is Case 1A, the Pacific surface duct at 300 Hz, where normal mode methods would be expected to have difficulties. Calculations were performed using the surface duct only with a half-space (ρ = 1, c = 1539.24 m/s) below 152.4 m, as well as for the entire profile with phase velocities confined to the range 1536 m/s to 1539.24 m/s. Fig. 4(a) shows that the effect of using the whole profile is to reduce the propagation loss somewhat, and to cause the nulls to be somewhat filled in. No computational difficulties were encountered in spite of the two-duct nature of the profile and the higher frequency than Case 2.

There is a benchmark result [Stickler, 1975] for Case 3B where there is only one trapped mode, near cutoff. In this case, the continuous spectrum, neglected in our model, is important. Our results agree with Stickler's results when he excludes the contribution of the continuous spectrum.

4.2 Mode Attenuation Coefficients

The AESD test cases discussed in Sec. 4.1 did not include any loss mechanisms, other than geometrical spreading. Fig. 5 shows the attenuation coefficients of mode 1 as a function of frequency for the AESD Test Case 3. The following parameters were used for the calculations:

Bottom absorption coefficient α	= 0.2 dB/m-kHz
Surface roughness σ_0	= 0.2 m
Bottom roughness σ_1	= 0.2 m
Shear speed in bottom c_s	= 200 m/s
Shear wave absorption coefficient α_s	= 1 dB/m-kHz.

The PRLOSS/NORMOD model [MacEachern, 1983] was used for these calculations, since the individual modal attenuation coefficients were readily available and it was possible to do multiple frequencies conveniently.

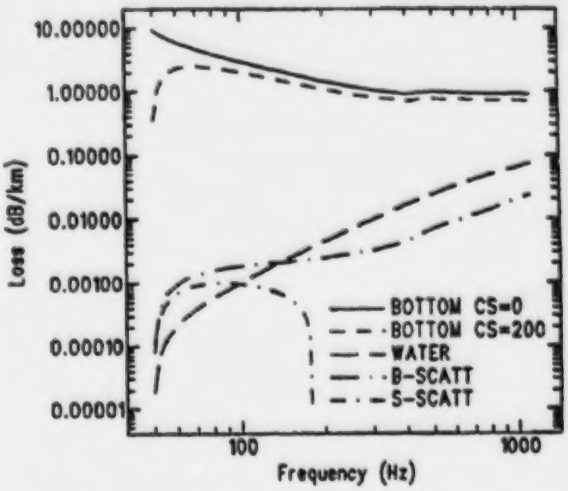

Fig. 5. Attenuation coefficients of mode 1 for AESD Test Case 8 with various assumed loss mechanisms: BOTTOM CS = 0 [Eq. (13) with $c_s = 0$]; BOTTOM CS = 200 [Eq. (19)]; WATER [Eq. (15)]; B-SCATT [Eq. (17)]; and S-SCATT [Eq. (16)].

Note that all the losses, except the bottom loss calculated by the perturbation formula, Eq. (13), approach 0 as the frequency approaches cutoff from above 50 Hz. The surface scattering loss increases to a maximum near 80 Hz, then decreases to 0 near 180 Hz when the phase velocity of mode 1 becomes less than the sound speed at the surface. At high frequencies the volume absorption in the water and the bottom scattering loss behave as f^2. The bottom loss decreases with increasing frequency since the grazing angle becomes smaller and the mode function does not penetrate as deeply into the bottom.

Notice that the losses with shear waves included are less than the losses with $c_s = 0$. Further calculations show that the effect of shear waves is negligible here since the bottom is so lossy anyway. The problem is that the two formulae for calculating bottom losses, Eqs. (13) and (19), are inconsistent, a problem that needs further investigation.

4.3 Group Velocities and Mode Functions

The group velocity rather than the phase velocity determines the speed at which energy is transported for a broadband signal. For a multilayered environment, the group velocity of each mode can show a rather complicated frequency dependence with several local minima and maxima. Chapman and Ellis [1983a] have shown that the mode functions can be used to give an intuitive understanding of the group velocity.

Figs. 6a and 6b [Chapman and Ellis, 1983a] show group velocity curves and mode functions for mode 5 in a three layer model: water, $\rho_1 = 1$, $h_1 = 100$ m, $c_1 = 1500$ m/s; silt, $\rho_2 = 1$, $h_2 = 100$ m, $c_2 = 1650$ m/s; rock, $\rho_3 = 2$, $h_3 = \infty$, $c_3 = 4500$ m/s, where the h_1 refer to layer thicknesses. The maxima in the group velocity curves at 50 and 73 Hz correspond to a "resonance" in the silt layer. The maximum near cutoff at 18.92 Hz occurs because most of the normalization of the mode function occurs in the high-speed rock layer. The minima near 20 and 90 Hz occur when the equivalent ray angle in the silt or water is nearing the critical angle with the higher speed layer below. The higher speed layer does not contribute enough to increase the group velocity however.

The group velocity and mode functions were calculated using the PROLOS/MODES program and some small utility programs.

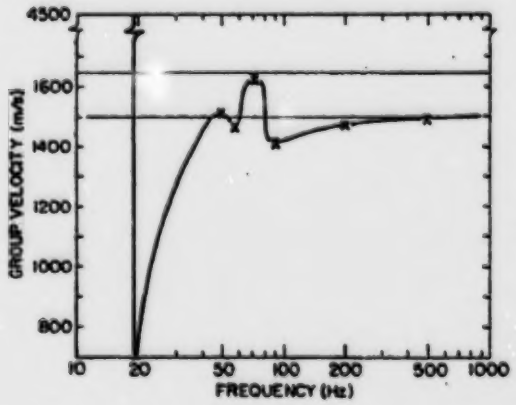

Fig. 6a. Group velocity versus frequency for mode 5 for a three-layer model. Symbols refer to mode plots in Fig. 6b.

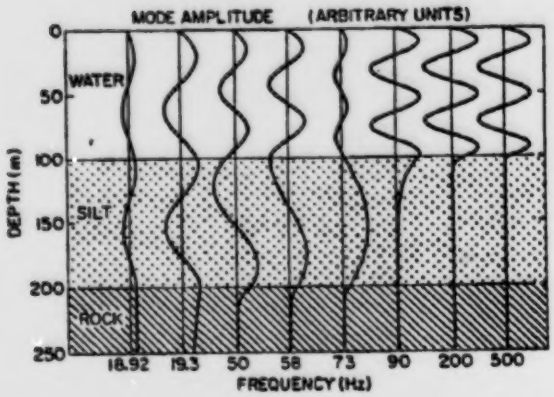

Fig. 6b. Amplitude of mode 5 as a function of depth for the three-layer model. The frequencies correspond to the points marked (x) in Fig. 6a.

4.4 Comparison With Shallow Water Data

It is usually much more difficult to obtain good agreement with experimental results than with other models. In shallow water the main difficulty is in obtaining accurate environmental information, particularly about the sea bed, for input to the model.

Fig. 7 shows a comparison of propagation loss predictions with measurements at a shallow water site. The measurements were made in summer conditions in a range-dependent environment with water depth varying between 115 and 155 m, and a sandy sediment layer overlying a semi-consolidated bottom. The sediment properties were obtained from an independent geo-acoustic model based on the analysis of a vertical incidence seismic profiler. The calculations were done by the adiabatic range-dependent normal mode model PROLOS. There is good agreement between the model and measurements at practically all ranges and frequencies. This shows about the best agreement that one is likely to obtain in shallow water, and is especially gratifying since it was not necessary to tune the geo-acoustic parameters to improve the fit. More details about the model and experiment are given by Ellis and Chapman [1984].

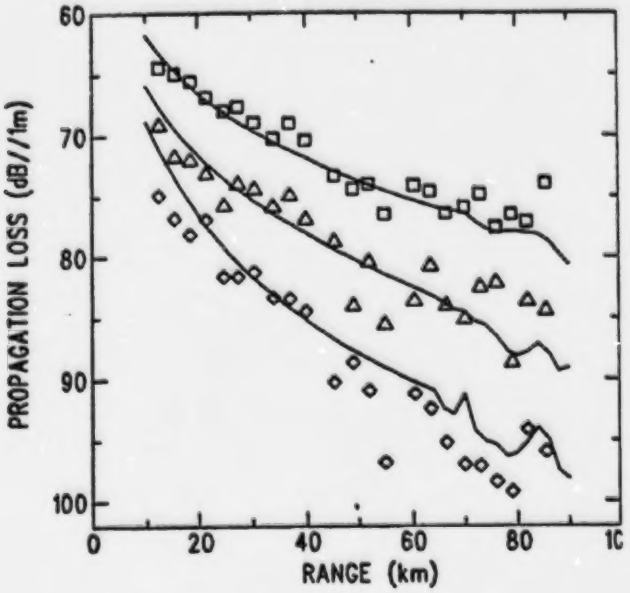

Fig. 7. Measured and modelled propagation loss versus range for a range dependent shallow water site. Measured: □ 64 Hz, Δ 256 Hz, ◇ 1024 Hz. Modelled: solid lines.

4.5 Discussion

In addition to the results shown earlier in this section, the two-ended shooting technique has been used extensively in shallow water calculations at DREA since 1979; in addition to the papers quoted earlier in this section see: [Ellis and Chapman, 1980], [Chapman, 1980], [Chapman, 1983], [Chapman and Ellis, 1983] as well as various other DREA reports. The method has worked successfully on all shallow water profiles and bottom models that we have tried and at frequencies up to 3000 Hz. This is not to say that we have always been able to get good agreement with our experimental measurements; but rather that the environmental inputs are inaccurate or the model does not account for certain phenomena.

One specific thing that is lacking is the ability to handle shear waves when the bottom is hard (e.g. granite with $c_s \sim 3000$ m/s) or consolidated (e.g. limestone or chalk with $c_s \sim 1000$ m/s). In the former case our algorithm could easily be generalized to handle a bottom half-space since it would only involve a change in the boundary condition at z_b. In the latter case the shear speed is too high for perturbation techniques to be applied, and the mode functions and wave numbers would be complex since $c_s < c(z)$ for z in the water. See [Ellis and Chapman, 1984] for more discussion.

In deep water the model neglects the continuous spectrum (or equivalently the steep rays) which may be important at short ranges. As well, the computation time increases since the number of modes is proportional to water depth. Other techniques such as the fast field method or parabolic equation may be more attractive. However, if long range propagation results are required, normal mode theory is often adequate or preferable. In such cases the algorithm would be quite useful, especially if a restricted range of phase velocities is all that needs to be computed. Since a two-ended shooting technique is used, the high sound speed near the surface is not a problem, as would be the case in single-ended shooting methods; the only problem that seems to arise (in range-independent cases) is in the two duct problems such as AESD Case 2 where there are two strong, well isolated sound channels. In such cases a multiple shooting technique or a finite difference approach might have to be used rather than the method described here.

5. SUMMARY AND CONCLUSIONS

We have described a two-ended shooting method that has been used for normal mode calculations at DREA since 1978. It is a technique borrowed from quantum mechanical calculations and generalized to handle density changes.

For completeness we have included loss mechanisms needed to compare model predictions with experiment, and have shown a variety of results. These include propagation loss calculations for standard test cases, mode functions and group velocities, model-data comparisons, and attenuation losses due to surface and bottom volume absorption, surface and bottom roughness, and shear wave losses in the bottom. Ways in which the method could be extended or improved are also discussed.

The method has been successfully applied to all shallow water profiles that we have attempted, and at frequencies up to 3000 Hz. We have not always obtained good agreement with experimental measurements, but this seems to be due to inaccuracies in the environmental information or the fact that our model does not account for certain things (e.g. high speed shear waves in the bottom).

In deep water environments the model usually performs well, although it of course neglects the continuous spectrum (or equivalently, the steep rays) which may be important at short ranges. Well isolated sound channels (such as the AESD Workshop Test Case 2) can cause some of the mode functions to be inaccurate at frequencies above 100 Hz. On the other hand, the algorithm using the layered environmental model has no trouble with AESD Test Case 1A, a surface duct at 300 Hz, even when the complete profile is used.

ACKNOWLEDGEMENTS

The basic algorithm and code for PROLOS/MODES were developed with Brian Leverman during his two terms as a Summer Research Assistant at DREA in 1978 and 1979.

The encouragement and feedback from the Shallow Water Acoustics Group were instrumental in the further development and refinement of the model to aid in the interpretation of their data. The continued interactions with my colleague D.M.F. Chapman were especially valuable.

The newer code PRLOSS/NORMOD was developed in 1982-83 primarily by Tim MacEachern of Wycove Systems Limited under DSS Contract 8AE81-00153. His comments on an earlier version of this manuscript are appreciated. Further work (1984) on the shear wave perturbation formula was performed by Brian Leverman, this time employed by Wycove Systems Limited, under DSS Contract 8SC83-00576.

Appendix A: Notation

$\underline{x}$	space co-ordinate (x,y,z) or (r,z,Θ)
$\underline{x}_o$	position of source $(0,z_o,0)$
r	range co-ordinate
z	depth co-ordinate
ρ	density
ρ_w	density of water
c	sound speed
f,ω	frequency, angular frequency $\omega=2\pi f$
t	time
P	pressure
u_n	mode function
h, h_l	water depth, layer thickness
$H_o^{(1)}$	Hankel function of zeroth order and first kind
k	wave number
k_n	wave number of the n-th discrete normal mode
δ_n	imaginary part of the wave number of the n-th mode
K_n	complex wave number of the nth mode; $K_n = k_n + i\delta_n$
c_m	minimum sound speed
c_B	sound speed in bottommost layer
S	source strength
PL	propagation loss in dB
IPL	incoherent propagation loss in dB

δ_{mn}	Kronecker delta
α	attenuation coefficient (dB/length at 1 kHz)
ϵ	attenuation coefficient (nepers/length)
σ_0, σ_1	r.m.s. heights of rough surface and bottom
R	plane wave reflection coefficient
$\gamma_n(z)$	local vertical wave number
$\beta_1, \beta_2, \beta_3$	vertical wave numbers used to determine reflection coefficient
$v_g^{(n)}$	group velocity of mode n
$I(z)$	phase or exponent integral
ϕ	phase shift at a mode turning point
z_1, z_2	upper and lower turning points of mode function
z_a, z_b	upper and lower limits for the numerical integration of the d.e.
z_m	matching depth for the two-ended shooting method

Dimensionless Variables

$x = z/h$	normalized depth
$V(x) = [h\omega/c(z)]^2$	dimensionless sound speed
$Q_n = h^2 k_n^2$	dimensionless eigenvalue
$w_n = h^{1/2} u_n$	dimensionless eigenfunction
$w_n' = \frac{dw_n}{dx} = h^{3/2} \frac{du_n}{dz}$	dimensionless derivative
$s(x) = \rho(z)/\rho_w$	dimensionless density

Appendix B: Absorption as a Perturbation

If absorption is introduced into the medium, the plane wave becomes attenuated; that is,

$$e^{ikr} \rightarrow e^{ikr} e^{-cr} \tag{B-1}$$

where c is the attenuation coefficient in nepers per unit distance. This is equivalent to letting the local wave number of the sound speed become complex; that is,

$$k(z) = \omega/c(z) + i\, c(z) . \tag{B-2}$$

The corresponding normal mode wave number also becomes complex:

$$K_n = k_n + i\, \delta_n . \tag{B-3}$$

The imaginary part of δ_n can be obtained by a perturbation calculation, in which the squares of small quantities are neglected. We start with the normal mode equation:

$$\rho(z) \frac{d}{dz}\left[\frac{1}{\rho(z)} \frac{du_n(z)}{dz}\right] + [k^2(z) - K_n^2]\, u_n(z) = 0 . \tag{B-4}$$

First, we multiply Eq. (B-4) by $[\rho(z)]^{-1} u_n^*(z)$, where u_n^* is the complex conjugate of u_n. Then we take the complex conjugate of Eq. (B-4) and multiply it by $[\rho(z)]^{-1} u_n(z)$. Next, subtract the two equations and integrate from zero to infinity, giving:

$$\int_0^\infty \left[u_n^*(z) \frac{d}{dz}\left(\frac{1}{\rho(z)} \frac{du_n}{dz}\right) - u_n(z) \frac{d}{dz}\left(\frac{1}{\rho(z)} \frac{du_n^*(z)}{dz}\right)\right] dz$$

$$+ \int_0^\infty \{[k^2(z) - k^{*2}(z)] - (K_n^2 - K_n^{*2})\} \frac{u_n(z) u_n^*(z)}{\rho(z)}\, dz = 0. \tag{B-5}$$

The integrand of the first equation can be written:

$$\frac{d}{dz}\left[\frac{u_n^*(z)}{\rho(z)} \frac{du_n}{dz} - \frac{u_n(z)}{\rho(z)} \frac{du_n^*(z)}{dz}\right] \tag{B-6}$$

and since $u_n(0)=0$, and $\lim u_n(z) \rightarrow 0$, the integral is zero. Also, if the imaginary parts of k(z) and K_n are small,

$$K_n^2 - K_n^{*2} = 4i k_n \delta_n \tag{B-7}$$

$$k^2(z) - k^{*2}(z) = 4i \omega\varepsilon(z)/c(z) . \tag{B-8}$$

Therefore from Eqs. (B-5)-(B-7), we obtain:

$$\delta_n = \frac{\omega}{k_n} \frac{\int_0^\infty \frac{\varepsilon(z) u_n(z) u_n^*(z)}{\rho(z)\, c(z)}\, dz}{\int_0^\infty \frac{u_n(z)\, u_n^*(z)}{\rho(z)}\, dz} . \tag{B-9}$$

If the mode functions are approximated by their unperturbed values, the integral in the denominator is just the normalization (unity). Moreover, if the unperturbed mode functions are used, the integrand of the first integral in Eq. (B-5) is zero everywhere, and not only at the end points. The attenuation due to absorption in any layer is given by

$$\delta_n^i = \frac{\omega}{k_n} \int_{z_{i-1}}^{z_i} \frac{\varepsilon(z)\, u_n^2(z)}{\rho(z)\, c(z)}\, dz . \tag{B-10}$$

For bottom absorption $z_{i-1} = h$, and $z_i = \infty$.

The above formula can also be used to calculate the volume absorption due to the water, by using 0 and h as the limits of the integration.

For an infinite half-space in the bottom (i.e. the bottommost layer),

$$u_n(z) = u_n(h) \exp[-\gamma_n(z-h)], \quad z>h \tag{B-11}$$

$$\int_h^\infty u_n^2(z)\, dz = \frac{u_n^2(h)}{2\gamma_n} \tag{B-12}$$

$$\therefore \delta_n^B = \frac{\omega}{2k_n} \frac{\varepsilon_B\, u_n^2(h)}{\gamma_n \rho_B c_B} \tag{B-13}$$

Appendix C: Iteration Procedure for the Two-Ended Shooting Method

The variational principle tells us that if we have a differential equation of the form:

$$H(x)\, u_n(x) = \lambda_n u_n(x) \tag{C-1}$$

where H is some differential operator, and v_n is a trial eigenfunction satisfying the appropriate boundary conditions, then an approximation Q_n to λ_n is given by:

$$Q_n = \frac{\int \frac{1}{\rho(x)}\, v_n(x)\, H(x)\, v_n(x)\, dx}{\int \frac{1}{\rho(x)} v_n^2(x)\, dx} \tag{C-2}$$

where $\rho(x)$ is the appropriate weighting function and the integral is performed over the interval of the boundary value problem.

In the two-ended shooting method, we have a trial function $v_n(z)$ which satisfies the normal mode equation:

$$\{ \frac{d}{dz} [\frac{1}{\rho(z)} \frac{d}{dz}] + \frac{1}{\rho(z)} \frac{\omega}{c^2(z)} \}\, v_n(z) = Q_n \frac{v_n(z)}{\rho(z)} \tag{C-3}$$

on the two intervals $o \le z < z_m$, and $z > z_m$, that is, everywhere except at z_m. Q_n is the trial approximation to the solution k_n^2. The function $v_n(z)$ is continuous, but $[\rho(z)]^{-1} v_n'(z)$ is discontinuous at $z = z_m$. By taking H(x) to be the quantity {....} in Eq. (C-3), we can use Eq. (C-2) to obtain a better approximation Q_n':

$$Q_n' = \int_o^{z_m^-} v_n(z)\, H(z)\, v_n(z)\, dz + \int_{z_m^+}^{\infty} v_n(z)\, H(z)\, v_n(z)\, dz$$

$$+ \int_{z_m^-}^{z_m^+} v_n(z)\, H(z)\, v_n(z)\, dz\,. \tag{C-4}$$

For notational simplicity in Eq. (C-4) the function $v_n(z)$ has been assumed to be normalized to unity, so the denominator term is absent. Since $H(z)v_n(z) = Q_n v_n(z)$ on the intervals $0 < z < z_m$ and $z > z_m$, the first two integrals can be evaluated to give:

$$I_1 + I_2 = Q_n \int_0^\infty \frac{v_n^2(z)}{\rho(z)}\, dz = Q_n \,. \qquad \text{(C-5)}$$

The final integral of Eq. (C-4), although integrated over an infinitesmally small interval, gives a finite contribution due to the presence of the derivatives in H(z). It can be evaluated using integration by parts to give:

$$\int_{z_m^-}^{z_m^+} v_n(z) \frac{d}{dz}\left[\frac{1}{\rho(z)} \frac{dv_n}{dz}\right] dz = \frac{v_n(z)}{\rho(z)} \frac{dv_n}{dz}\Big|_{z_m^-}^{z_m^+} - \int_{z_m^-}^{z_m^+} \frac{1}{\rho(z)} \left[\frac{dv_n}{dz}\right]^2 dz \,. \qquad \text{(C-6)}$$

Since the integral term on the r.h.s. of Eq. (C-6) is negligible, the improved estimate Q_n is given by:

$$Q'_n = Q_n + \frac{v_n(z_m)\left\{\frac{1}{\rho(z_m^+)} \frac{dv_m(z_m^+)}{dz} - \frac{1}{\rho(z_m^-)} \frac{dv_m(z_m^-)}{dz}\right\}}{\int_0^\infty \frac{v_n^2(z)}{\rho(z)}\, dz} \,. \qquad \text{(C-7)}$$

In Eq. (C-7), the denominator has been re-introduced so the expression can be used with trial functions which are not normalized.

Appendix D: Dimensionless Co-ordinates

It is often useful for numerical purposes to define the variables in terms of dimensionless quantities. The calculations can then be done independently of the units used.

A dimensionless depth co-ordinate can be defined in terms of the water depth h as:

$$x = z/h \, . \tag{D-1}$$

If the following definitions are made:

$$V(x) = [h\omega/c(hx)]^2 \tag{D-2}$$

$$Q_n = h^2 k_n^2 \tag{D-3}$$

$$s(x) = \rho(hx)/\rho_w \tag{D-4}$$

then the normal mode Eq. (6) can be written:

$$s(x) \frac{d}{dx} \left[\frac{1}{s(x)} \frac{dw_n}{dx} \right] + [V(x) - Q_n] w_n(x) = 0 \tag{D-5}$$

where the w_n are the new normal mode functions normalized so that:

$$\int_0^\infty s^{-1}(x) w_n^2(x) \, dx = 1 \, . \tag{D-6}$$

In terms of the dimensionless mode functions:

$$u_n(hx) = \rho_w^{-1} h^{-1/2} w_n(x) \tag{D-7}$$

$$\frac{du_n(hx)}{dz} = \rho_w^{-1} h^{-3/2} \frac{dw_n(x)}{dx} \, . \tag{D-8}$$

The constraints on the eigenvalues become:

$$\frac{h\omega}{c_m} > Q_1 > Q_2 > \ldots > Q_N > \frac{h\omega}{c_B}. \qquad \text{(D-9)}$$

The number of modes, of course, does not change.

The boundary conditions do not change, so $w_n(0) = 0$, w_n and $\rho^{-1}w_n'$ are continuous, and the behaviour of w_n for large x is:

$$w_n(x) \sim \exp(-g_n x) \qquad \text{(D-10)}$$

where,

$$g_n = [Q_n - \frac{h^2\omega^2}{c_B^2}]^{1/2}. \qquad \text{(D-11)}$$

The iteration formula for the eigenvalues can be written as:

$$Q_n^{new} = Q_n^{old} + \frac{w_n(x_m)[\frac{w_n'(x_m^+)}{s(x_m^+)} - \frac{w_n'(x_m^-)}{s(x_m^-)}]}{\int_0^\infty \frac{w_n^2(x)}{s(x)}\,dx}. \qquad \text{(D-12)}$$

REFERENCES

[Bartberger and Ackler, 1973]
C.L. Bartberger and L.L. Ackler, "Normal mode solutions and computer programs for underwater sound propagation", NADC/AESD Reports NADC-72001-AE and NADC-72002-AE, April 1973.

[Blatt, 1967]
J.M. Blatt, "Practical points concerning the solution of the Schrodinger equation", J. Comp. Physics, 1, 382-396 (1967).

[Brekhovskikh, 1980]
L.M. Brekhovskikh, Waves in Layered Media, 2nd Ed., Academic Press, 1980, pp. 43-47.

[Chapman, 1980]
D.M.F. Chapman, "The directional nature of attenuation of sound due to scattering at a rough ocean surface", J. Acoust. Soc. Am. 68, 1475-1481 (1980).

[Chapman, 1983]
D.M.F. Chapman, "An improved Kirchoff formula for reflection loss at a rough ocean surface at low grazing angles", J. Acoust. Soc. Am. 73, 520-527 (1983).

[Chapman and Ellis, 1983a]
D.M.F. Chapman and D.D. Ellis, "The group velocity of normal modes", J. Acoust. Soc. Am., 74, 973-79 (1983).

[Chapman and Ellis, 1983b]
D.M.F. Chapman and D.D. Ellis, "Geo-acoustic models for propagation modelling in shallow water", Canadian Acoustics, 11(2), April 1983, 9-24.

[Ellis, 1982]
D.D. Ellis, "Some simple formulae for normal mode wave numbers, cutoff frequencies, and the number of modes trapped by a sound channel", Canadian Acoustics, 10(4), October 1982, pp. 7-15. Also, DREA Technical Memorandum 82/O, November 1982.

[Ellis and Chapman, 1980]
D.D. Ellis and D.M.F. Chapman, "Propagation loss modelling on the Scotian Shelf: Comparison of results with experiment", in Bottom-Interacting Ocean Acoustics, W.A. Kuperman and F.B. Jensen, Eds., Plenum Press, New York, 1980, pp. 541-555.

[Ellis and Chapman, 1984]
D.D. Ellis and D.M.F. Chapman, "Modelling of shear-wave related acoustic propagation on the UK continental shelf", DREA Technical Memorandum 84/P, August 1984.

[Ellis and Leverman, 1982]
D.D. Ellis and B.A. Leverman, "Software documentation for the normal mode subprogram: MODES", DREA Research Note AM/82/4, June 1982. Informal communication.

[Hamilton, 1972]
E.L. Hamilton, "Compressional wave attenuation in marine sediments", Geophysics, 37, 620-646 (1972).

[Hamilton, 1974]
E.L. Hamilton, "Geoacoustic models of the sea floor", in Physics of Sound in Marine Sediments, Loyd Hampton, Ed., 181-221, 1974, Plenum Press.

[Jensen and Ferla, 1979]
F.B. Jensen and M.C. Ferla, "SNAP, The SACLANTCEN normal-mode acoustic propagation model", SACLANTCEN Memorandum SM-121, January 1979.

[Koch et al, 1983]
R.A. Koch, C. Penland, P.J. Vidmar, K.E. Hawker, "On the calculation of normal mode group velocity and attenuation", J. Acoust. Soc. Am., 73, 820-825 (1983).

[Kuperman and Ingenito, 1977]
W.A. Kuperman and F. Ingenito, "Attenuation of the coherent component of sound propagation in shallow water with rough boundaries", J. Acoust. Soc. Am. 61, 1178-1187 (1977).

[Leverman, 1982]
B.A. Leverman, "User's guide to the normal mode propagation-loss package PROLOS", DREA Research Note, AM/82/3, June 1982. Informal communication.

[MacEachern, 1983]
T. MacEachern, "NORMOD/PRLOSS acoustic propagation loss calculation system", DREA Contractor Report, Wycove Systems Ltd., December 1983.

[Pierce, 1965]
A.D. Pierce, "Extension of the method of normal modes to sound propagation in an almost-stratified medium", J. Acoust. Soc. Am. 37, 19-27 (1965).

[Schiff, 1968]
L.J. Schiff, Quantum Mechanics, McGraw Hill, 1968, pp. 268-279.

[Spofford, 1978]
C.W. Spofford, "A synopsis of the AESD (Acoustic Environmental Support Detachment) workshop on acoustic-propagation modeling by non-ray-tracing techniques, 22-25 May 1978", Washington, D.C., AESD-TN-78-05, November 1978.

[Stickler, 1975]
D.C. Stickler, "Normal mode program with both the discrete and branch line contributions", J. Acoust. Soc. Am. 57, 856-861 (1975).

[Thorpe, 1967]
W.H. Thorpe, "Analytic description of the low-frequency attenuation coefficient", J. Acoust. Soc. Am., 42, 270 (1967).

[Tolstoy, 1956]
I. Tolstoy, "Resonant frequencies and high modes in layered wave guides", J. Acoust. Soc. Am. 28, 1182-1192 (1956).